THE JOURNAL OF BIOLOGICAL CHEMISTRY
Vol. 278, No. 42, Issue of October 17, pp. 41294–41301, 2003

Printed in U.S.A.

Endothelin-1 Decreases Gap Junctional Intercellular Communication by Inducing Phosphorylation of Connexin 43 in Human Ovarian Carcinoma Cells*

Received for publication, May 7, 2003, and in revised form, August 1, 2003
Published, JBC Papers in Press, August 7, 2003, DOI 10.1074/jbc.M304785200

Francesca Spinella‡, Laura Rosanò, Valeriana Di Castro, Maria Rita Nicotra§, Pier Giorgio Natali¶, and Anna Bagnato‖

From the Laboratories of Molecular Pathology and Ultrastructure and ¶Immunology, Regina Elena Cancer Institute, Rome 00158, Italy and the §Institute of Molecular Biology and Pathology, National Research Council, Rome 00137, Italy

Endothelin-1 (ET-1) is overexpressed in ovarian carcinoma and acts as an autocrine factor selectively through the ET_A receptor (ET_AR) to promote tumor cell proliferation, survival, neovascularization, and invasiveness. Loss of gap junctional intercellular communication (GJIC) is critical for tumor progression by allowing the cells to escape growth control. Exposure of HEY and OVCA 433 ovarian carcinoma cell lines to ET-1 led to a 50–75% inhibition in intercellular communication and to a decrease in the connexin 43 (Cx43)-based gap junction plaques. To investigate the phosphorylation state of Cx43, ovarian carcinoma cell lysates were immunoprecipitated and transient tyrosine phosphorylation of Cx43 was detected in ET-1-treated cells. BQ 123, a selective ET_AR antagonist, blocked the ET-1-induced Cx43 phosphorylation and cellular uncoupling. Gap junction closure was prevented by tyrphostin 25 and by the selective c-Src inhibitor, PP2. Furthermore, the increased Cx43 tyrosine phosphorylation was correlated with ET-1-induced increase of c-Src activity, and PP2 suppressed the ET-1-induced Cx43 tyrosine phosphorylation, indicating that inhibition of Cx43-based GJIC is mainly mediated by the Src tyrosine kinase pathway. *In vivo*, the inhibition of human ovarian tumor growth in nude mice induced by the potent ET_AR antagonist, ABT-627, was associated with a reduction of Cx43 phosphorylation. These findings indicate that the signaling mechanisms involved in GJIC disruption on ovarian carcinoma cells depend on ET_AR activation, which leads to the Cx43 tyrosine phosphorylation mediated by c-Src, suggesting that ET_AR blockade may contribute to the control of ovarian carcinoma growth and progression also by preventing the loss of GJIC.

The endothelin (ET)[1] family is composed of three isopeptides, ET-1, -2, and -3, that are potent mitogens for several human tumors, including carcinoma of the prostate (1), ovary (2, 3), colon (4), cervix (5), breast (6), and endometrium (7) as well as melanoma (8) and Kaposi's sarcoma (9). ETs and their receptors have been implicated in tumor progression through autocrine and paracrine pathways. ET-1 is produced primarily by vascular cells and in elevated amounts by different tumor cells and acts through two distinct subtypes of G protein-coupled receptors (GPCR), namely ET_A receptor (ET_AR) and ET_BR, that have different affinities for ETs (10). The ET-1/ET_AR autocrine pathway has a key role in the development and the progression of prostatic, ovarian, and cervical cancers (11).

We have previously demonstrated that ET-1 and ET_AR are overexpressed in primary and metastatic ovarian carcinomas compared with normal ovarian tissues (3). In ovarian tumor cells, ET-1 acts an autocrine factor selectively through ET_AR (2). Ligand binding to this receptor results in activation of a pertussis toxin-insensitive G protein that stimulates phospholipase C activity and increases intracellular Ca^{2+} levels, activation of protein kinase C, mitogen-activated protein kinase, and p125 focal adhesion kinase phosphorylation (11). In this tumor, engagement of ET_AR promotes tumor cell proliferation (3, 12), apoptosis protection (13), invasiveness (14), and neovascularization (15–17). ET_AR blockade by a selective receptor antagonist, ABT-627, inhibits tumor growth, angiogenesis, and metastasis-related effectors of ovarian carcinoma *in vivo* (18).

Recent evidence shows that ET-1 has also been implicated in the regulation of gap junctions in astrocytes, Rat-1 and cardiac cells, although the mechanism that regulates this effect has not been fully established (19–21). Moreover, the role of ET-1 in the regulation of GJIC in tumor cells has not been studied.

GJs are composed of transmembrane channel proteins, termed connexins (Cxs), that directly connect the cytoplasm of two adjacent cells, allowing the cells to review and shape the functional state of their neighbors by exchanging signaling molecules, a process called gap junctional intercellular communication (GJIC) (22).

During the transition to malignant lesions and to metastatic cancer, stepwise changes in intercellular communications provide tumor cells with the ability to overcome microenvironmental controls from the host, to invade surrounding tissues, and to metastasize (23). Various tumor-promoting agents (24, 25) and different growth factors (26) decrease GJIC, either by suppressing Cx expression or by inducing post-translational modifications such as phosphorylation, a process that is closely related

* This work was supported by grants from the Associazione Italiana Ricerca sul Cancro, from Ministero della Salute, and from MIUR-Consiglio Nazionale delle Ricerche. The costs of publication of this article were defrayed in part by the payment of page charges. This article must therefore be hereby marked "*advertisement*" in accordance with 18 U.S.C. Section 1734 solely to indicate this fact.

‡ Recipient of a fellowship from Fondazione Italiana Ricerca sul Cancro.

‖ To whom correspondence and reprint requests should be addressed: Laboratory of Molecular Pathology and Ultrastructure, Regina Elena Cancer Institute, Via delle Messi d'Oro 156, Rome 00158, Italy. Tel.: 39-06-52662565; Fax: 39-06-52662505; E-mail: bagnato@ifo.it.

[1] The abbreviations used are: ET-1, endothelin-1; GJIC, gap junction intercellular communication; Cx, connexin; Cx43, connexin 43; ET_AR and ET_BR, endothelin receptor A and B, respectively; GPCR, G protein-coupled receptor(s); PP2, 4-amino-5-(4-chlorophenyl)-7-(*t*-butyl)pyrazolo[3,4-*d*]pyrimidine; LY, Lucifer Yellow; RhD, rhodamine-dextran; SL/DT, scrape loading/dye transfer; Ab, antibody; PBS, phosphate-buffered saline.

to cellular processes such as trafficking, assembly/disassembly, gating of gap junction channels, and altered susceptibility to degradation (27). Several studies have shown that the turnover of connexins is exceptionally rapid and that degradation of Cx43 involves both the lysosome and the proteasome pathways (28). Phosphorylation, in most cases, is a prerequisite for ubiquitination that marks the protein for proteasomal destruction. The COOH-terminal tail of Cx43 contains several serine and tyrosine phosphorylation sites, suggesting that this region of the molecule contains a complex array of potential regulatory sites (20).

Human ovarian surface epithelial cells exhibit extensive GJIC and expression of different types of Cx (*e.g.* Cx26, Cx32, and Cx43) (29–31). Defects in intercellular communication, including reduced or inappropriate expression of Cx43, the main gap junction protein in normal human ovarian surface epithelium, has emerged as key factors in ovarian carcinoma progression (29–33). The aim of this study was to examine whether the activation of the ET_AR by ET-1 leads to a reduction of Cx43-mediated GJIC in ovarian carcinoma cells and, if so, to determine the involved signaling pathways targeting Cx43. Because phosphorylation of Cx43 is believed to be causally linked with disruption of GJIC, we analyzed whether ET-1 could modulate the phosphorylation of Cx43. Using two ovarian carcinoma cell lines, HEY and OVCA 433, in which the ET-1/ET_AR autocrine pathway is biologically active, we report here for the first time in tumor cells that 1) ET-1 significantly decreases intercellular communication and Cx43 expression at the cell surface; 2) these activities require ET_AR activation; and 3) Cx43 phosphorylation is mainly mediated by the Src tyrosine kinase pathway. In addition, ABT-627 (atrasentan), a nonpeptide orally bioavailable ET_AR antagonist with *in vivo* and *in vitro* antitumor activity (18, 34–37), prevents *in vivo* Cx43-based GJIC loss of function. Thus, our findings identify the signaling pathways linking ET_AR with cellular uncoupling, which may contribute to ET-1-mediated ovarian tumor progression.

EXPERIMENTAL PROCEDURES

Cells—Human ovarian carcinoma cell lines HEY and OVCA 433 were a generous gift from Prof. G. Scambia (Catholic University School of Medicine, Rome, Italy) and were cultured in Dulbecco's modified Eagle's medium containing 10% fetal calf serum. When the cells reached 70–80% confluence, the cultures were serum-deprived by incubation for 24 h in Dulbecco's modified Eagle's medium in the absolute absence of serum. All culture reagents were from Invitrogen (Paisley, Scotland, UK). ET-1 (Peninsula Laboratories, Belmont, CA) was added in the HEY and OVCA 433 cell medium at the indicated concentration and for the indicated time. When the effects of the antagonists (BQ 123 and BQ 788; Peninsula Laboratories) were studied, they were added 15 min before agonist. Pretreatment of cells with pervanadate (1 mM), PP2 (50 nM), tyrphostin 25 (100 μM), or staurosporine (100 nM) (Calbiochem) was performed for 30 min prior to the addition of ET-1.

Scrape Loading/Dye Transfer—Levels of GJIC in control and treated cultures were determined using the scrape-loading/dye transfer (SL/DT) technique, applying a mixture of fluorescent dyes; Lucifer Yellow (LY) (Sigma) and rhodamine-dextran (RhD) (Molecular Probes, Inc., Eugene, OR) (38). HEY and OVCA 433 cells, cultured as described above, were washed thoroughly with PBS in which Ca^{2+} was omitted to prevent uncoupling of the cells due to high Ca^{2+}. The mixture containing 0.5% LY and 0.5% RhD in Ca^{2+}-free PBS was added to the cells, and scrape loading was performed, applying two or three cuts on cell monolayers with a razor blade. The dye mixture was rinsed away 1 min after the scrape. Cells were washed three times with PBS and fixed with 4% paraformaldehyde, and cells stained with LY and/or with RhD were detected by fluorescence emission with an inverted fluorescent microscope equipped with a camera. Junctional permeability was measured after the scrape by taking five successive images per trial. Cells that received the LY from the scrape-loaded cells, excluding the RhD-stained cells, were considered communicating. The numbers of communicating cells in the untreated and treated samples were counted. Gap junction communicating capacity was expressed as percentage of the control.

Immunostaining of Cx43—HEY cells were grown to 80% confluence in 8 wells of tissue culture (Labtek). After the addition of 100 nM ET-1 for 30 min, the cells were rapidly washed with ice-cold PBS and fixed on acetone. The cells were incubated overnight at 4 °C with mouse monoclonal anti-Cx43 (Chemicon International, Temecula, CA) diluted 1:10 in PBS and then for 1 h with a fluorescein-labeled goat anti-mouse IgG (Fab′) fraction (Cappel; ICN Biomedicals GmbH) diluted 1:200 in PBS at room temperature. Cells stained directly with the secondary antibody or with the isotype-matched murine immunoglobulins were used as a negative control. Indirect immunofluorescence staining was carried out on acetone-fixed 4-μm frozen tissue sections employing rabbit anti-Cx43 antiserum and fluorescein-labeled goat anti-rabbit IgG (Fab′) fraction (Sigma).

Immunoprecipitation and Immunoblotting—Cells were washed with ice-cold PBS and lysed in lysis buffer (50 mM Tris-HCl (pH 7.4), 250 mM NaCl, 50 mM sodium fluoride, 5 mM EDTA, 0.15% Triton X-100, 1 mM orthovanadate, 0.06 units of aprotinin, 1 mM phenylmethylsulfonyl fluoride, and 10 μg/ml leupeptin). For immunoprecipitation of Cx43, cells were lysed in lysis buffer. Cell lysates, obtained after centrifugation at 14,000 $\times$ *g* for 10 min to remove insoluble material, were incubated overnight at 4 °C with protein A-Sepharose (Amersham Biosciences). Immunoprecipitation was performed by incubation overnight at 4 °C of the precleared lysates with a polyclonal anti-pan-Cx43 antibody (Santa Cruz Biotechnology, Inc., Santa Cruz, CA), which detects nonphosphorylated and phosphorylated Cx43 species, insolubilized on protein A-Sepharose. After washing six times with lysis buffer, the immunoprecipitated material was solubilized in 2$\times$ SDS Laemmli buffer under reducing conditions and analyzed by electrophoresis on 12.5% SDS-PAGE gels and transferred to nitrocellulose for immunoblotting. Nonspecific binding of Abs was prevented by incubating the blotted membrane in 3% bovine serum albumin TBS-T (10 mM Tris, pH 8.0, 150 mM NaCl, 0.05% Tween) for 1 h at room temperature. The blots were then incubated for 1 h with anti-phosphotyrosine or with anti-pan-c-Src, a nonphosphospecific antibody or with anti-c-Src ($Tyr(P)^{418}$) polyclonal antibody (BIOSOURCE) or anti-Cx43 monoclonal Ab (Transduction Laboratories). Membranes were then washed with TBS-T three times for 15 min each at room temperature and incubated for 1 h with peroxidase-conjugated secondary antibody, washed again, and subjected to the ECL (Amersham Biosciences).

For detection of Cx43 or c-Src or activated form of c-Src, an equal amount of cell lysate proteins from ovarian carcinoma cells or homogenized HEY tumor specimens was subjected to 12% SDS-PAGE and transferred to nitrocellulose. The filters were blocked with 3% bovine serum albumin in TBS-T and incubated with either Cx43 (Transduction Laboratories), anti-pan-c-Src (BIOSOURCE), or an activated form of c-Src (BIOSOURCE) antibodies for 1 h. After washing with TBS-T, blots were incubated with appropriate peroxidase-conjugated secondary antibody, washed again, and subjected to the ECL (Amersham Biosciences) procedure. After being stripped, the membranes were reprobed with β-actin monoclonal antibody (Oncogene, CN Biosciences, Inc., Darmastadt, Germany) to ensure equal loading. The relative intensity of signals was quantified using the Scion image analysis program. The quantification data was statistically analyzed using Student's *t* test and represent the average value of three independent Western blots.

HEY Xenografts in Nude Mice—Female athymic (nu^+/nu^+) mice, 4–6 weeks old, were purchased from Charles River Laboratories (Milan, Italy). The treatment protocol followed the guidelines of animal experimentation adopted by the Regina Elena Cancer Institute under the control of the Ministry of Public Health. Mice were given injections subcutaneously into one flank with 1.5×10^6 viable HEY cells, as determined by trypan blue staining, resuspended in 200 μl of PBS. After 7 days, when established tumors of ~0.2–0.3 cm^3 in diameter were detectable, mice were randomized in groups ($n = 10$) to receive different treatments. One group was treated intraperitoneally for 21 days with ABT-627 (atrasentan, provided by Abbott, at daily doses of 2 mg/kg/day) dissolved in 0.25 N $NaHCO_3$. Control mice were injected in the same way with 200 μl of drug vehicle. On day 40 after tumor injection, tumors were removed from control and treated mice and snap frozen in liquid nitrogen for immunohistochemical and Western blot analysis.

Statistical Analysis—All statistical analyses were assessed using a two-tailed Student's *t* test and were performed by the Instat software system (GraphPad Software Inc., San Diego, CA).

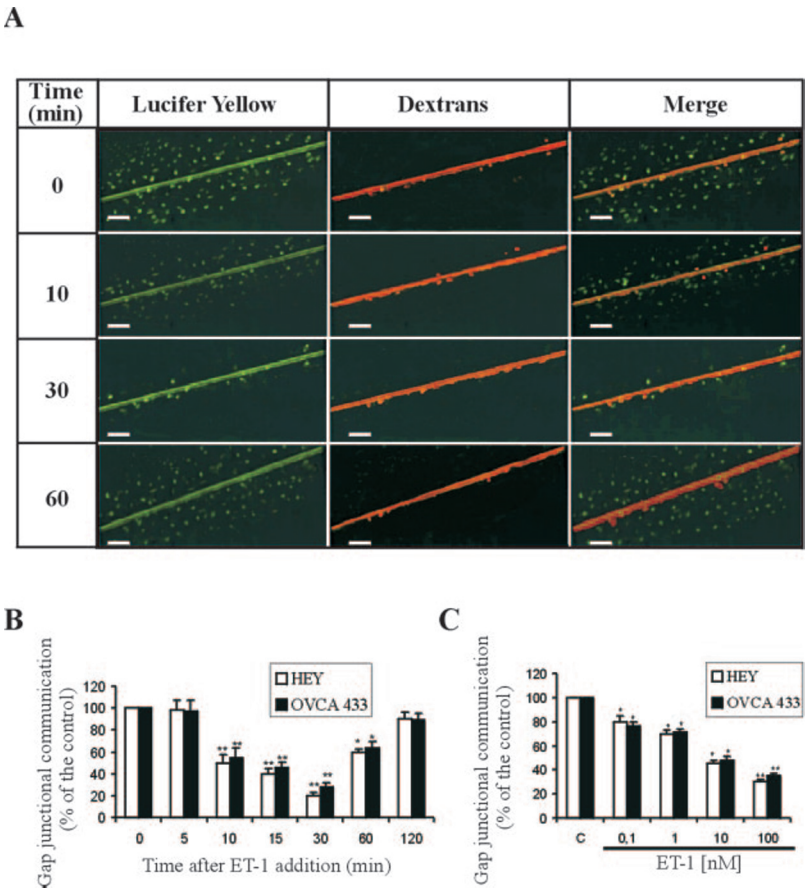

FIG. 1. **ET-1-induced GJIC inhibition in HEY and OVCA 433 ovarian carcinoma cells.** Cells were treated with 100 nM ET-1 for up to 120 min, and GJIC capacity was assayed by the SL/DT method. HEY and OVCA 433 cells were incubated at different times with 100 nM ET-1 (*A* and *B*) or with the indicated concentrations of ET-1 for 30 min (*C*), and GJIC function was evaluated by analyzing net transfer of LY, excluding dextran-stained cells, as described under "Experimental Procedures." The data, reported in *B* and *C* as the relative percentage of the control, show a representative experiment of three different experiments; results are means of triplicate samples ± S.D.; *, $p < 0.05$; **, $p < 0.001$ compared with control. *Bar* (*A*), 100 μm.

RESULTS

ET-1 Inhibits Gap Junctional Intercellular Communication in Ovarian Carcinoma Cells—Although previous studies demonstrated that ET-1 disrupted GJIC in astrocytes (19) and in Rat-1 cells (20), its effect on the regulation of GJIC in tumor cells has not been studied. Therefore, we evaluated the effect of ET-1 on GJIC of two ovarian carcinoma cell lines, HEY and OVCA 433, that express functional ET_AR and secrete high levels of ET-1 (3). We used the SL/DT method, applying a low molecular mass fluorescent tracer, LY, which transfers through the gap junction channel, to monitor GJIC function and RhD, which does not pass through the channels, to identify the incision sites or artificially damaged cells. For the evaluation of GJIC function, cells stained only with LY, excluding the RhD-stained cells, were counted. As assessed by the SL/DT technique, serum-starved ovarian carcinoma cells were communication-competent and transferred LY to several cells distant to the wound edge (Fig. 1). The addition of 100 nM ET-1 to the cell medium resulted in a transient and time-dependent reduction in GJIC. Intercellular movement of LY was still detectable 10 min after ET-1 addition, at this time inhibition of GJIC was 50%, whereas after 30 min the dye remained confined to the wounded cells, and GJIC were inhibited by 70–80% with respect to the controls. Ovarian cancer cell GJIC returned to basal levels within 2 h (Fig. 1*B*). After exposure to different concentrations of ET-1 for 30 min, a dose-dependent inhibition was detected in HEY and OVCA 433 cells. ET-1 at a dosage of 0.1 nM induced a 20% inhibition that reached 70% at a concentration of 100 nM ET-1 (Fig. 1*C*). In all of these experiments, the transmembrane permeability was not affected by agonist stimulation, since both stimulated and control cells showed negligible dye loss over a 3-h period. Thus, the observed inhibition of LY diffusion represented an ET-1-induced decrease in gap junctional communication.

ET-1 Induces Phosphorylation of Cx43—To determine whether ET-1 can regulate Cx43 expression in ovarian carcinoma cells, HEY and OVCA 433 cells were exposed for different times to ET-1 (100 nM). ET-1 significantly induced dose-dependent increase in the electrophoretic mobility shift of Cx43 (Fig. 2*A*). As analyzed by SDS-PAGE, Cx43 is normally reported as being represented by a faster migrating, nonphosphorylated species (Cx43-P_0) and two more slower migrating, phosphorylated species (Cx43-P1 and Cx43-P2) (39) that we refer to collectively as Cx43-P. ET-1 treatment resulted a in time-dependent Cx43 phosphorylation reaching the maximum level after 30 min and returning to basal level after 1 h of exposure to ET-1 (Fig. 2*A*). Treatment with alkaline phosphatase results in the total disappearance of the slower migrating bands, indicating that these bands correspond to the phosphorylated forms of Cx43 (Fig. 2*B*). The differences in Cx43 banding patterns between the two cell lines may reflect differential steady-state levels probably related to kinetic variability in Cx43 turnover. Nonphosphorylated Cx43 (Cx43-P_0) was detected in untreated HEY cells, whereas the phosphorylated Cx43 species (Cx43-P) were much less apparent (Fig. 2, *A* and *B*). Exposure of HEY cells to from 0.1 nM up to 100 nM ET-1 for 30 min resulted in a dose-dependent increase of Cx43 phosphorylation that reached the highest intensity at 100 nM of ET-1 (Fig. 2*C*). Densitometric analysis of Fig. 2*C* shows that ET-1 increased the Cx43-P at the expense of Cx43-P_0 (Fig. 2*D*, *left*), and the total cellular Cx43 content only slightly decreased following treatment with ET-1 (Fig. 2*D*, *right*).

We further examine the other connexin subtypes that participate in gap junction formation in HEY and OVCA 433 cells. Western blotting showed that Cx32 and Cx26 expression was barely detectable in these cells, and ET-1 did not modify their levels of expression (data not shown).

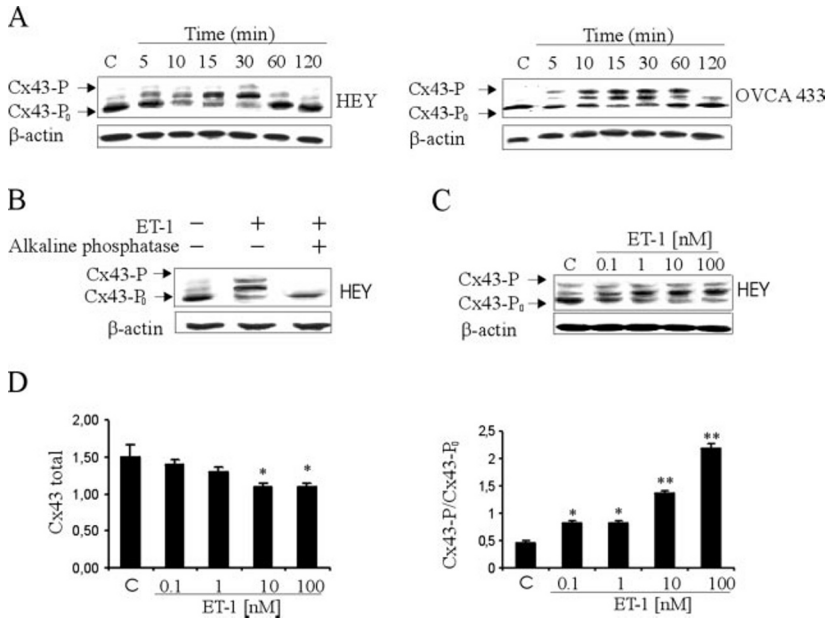

FIG. 2. **Effects of ET-1 on Cx43 expression in ovarian carcinoma cells.** HEY and OVCA 433 cells were stimulated for up to 120 min with 100 nM ET-1 (*A*). Samples from 30-min ET-1 (100 nM)-stimulated HEY cells were incubated with alkaline phosphatases treatment and analyzed for Cx43 expression by Western blotting (*B*). HEY cells were also stimulated with different concentrations of ET-1 for 30 min (*C*). Whole cell lysates were assayed for Cx43 expression by Western blotting with anti-Cx43. After being stripped, the membranes were reprobed with β-actin-specific antibody to ensure equal loading. The relative density of Cx43-P/Cx43-P_0 ratio and total Cx43 content (*D*) from HEY cells treated with different concentration of ET-1 (*B*) were statistically analyzed and represent the average value of three independent Western blots ± S.D. *, $p < 0.001$; **, $p < 0.05$ compared with untreated cells.

ET-1-induced Cx43 Phosphorylation and GJIC Inhibition Are Mediated through ET_AR—To investigate which receptor subtype mediates ET-1-induced disruption of GJIC and Cx43 phosphorylation, a selective ET_A receptor antagonist, BQ123, and a selective ET_BR antagonist, BQ788, were used in the presence or absence of 100 nM ET-1. BQ123 was able to completely block ET-1-induced Cx43 phosphorylation, whereas BQ 788 did not (Fig. 3*A*). To determine whether ET_AR was responsible for the inhibition of GJIC, BQ 123 was used in SL/DT experiments. ET-1-induced dye transfer inhibition was prevented by the ET_AR antagonist (Fig. 3*B*). Taken together, these findings indicate that ET-1 acts through ET_AR to induce the phosphorylation of Cx43 and to disrupt the GJIC.

ET-1 Alters the Localization of Cx43 Expression in Ovarian Carcinoma Cells—To examine the possibility that ET-1-induced Cx43 phosphorylation modified the distribution of membrane gap junction plaques, we investigated HEY cells with Cx43-specific antibody by indirect immunofluorescence. A fine punctate Cx43-specific staining characteristic of gap junctional plaques was observed often outlining cell boundaries of the untreated cells. After 30 min of ET-1 treatment, the fine punctate staining pattern was significantly reduced, now appearing as granular and randomly distributed (Fig. 4, *A* and *B*). This change was concomitant with the phosphorylation of Cx43 and the complete inhibition of dye transfer to adjacent cells.

ET-1-induced GJIC Reduction Is Regulated by Tyrosine Kinase Pathways—A number of kinases and signal transduction pathways are known to affect GJIC and Cx43 phosphorylation (26). To identify the kinase responsible for ET-1-induced GJIC reduction, we examined the effects of tyrosine and serine/threonine kinase and tyrosine-phosphatase inhibitors on GJIC activity. Pervanadate (1 mM), a tyrosine-phosphatase inhibitor, induced a complete inhibition of LY spreading between LY-loaded HEY cells by the same extent observed in ET-1-treated cells (Fig. 5). Conversely, ET-1-induced gap junction closure was fully prevented by tyrosine kinase inhibitor tyrphostin 25 (100 μM). These results suggest that tyrosine kinase pathways mainly regulate ET_AR-mediated gap junction closure in ovarian carcinoma cells. The serine/threonine kinase inhibitor, staurosporine (100 nM) only partially reversed the effect of ET-1 on GJIC (Fig. 5), suggesting that ET-1 can also phosphorylate Cx43 on serine residues after activation of several serine/threonine kinases, such as protein kinase C.

ET-1 Induces Tyrosine Phosphorylation of Cx43—To prove that the observed ET-1-induced phosphorylation of Cx43 occurs on tyrosine residue, we performed immunoprecipitation and immunoblot experiments with anti-Cx43. HEY cells were incubated for increasing time periods with 100 nM ET-1, and cell lysates were immunoprecipitated with anti-Cx43 and immunoblotted with anti-phosphotyrosine (Fig. 6*A*). Immunoblot analysis indicated that ET-1 treatment resulted in a time-dependent induction of Cx43 tyrosine phosphorylation. Fig. 6*B* shows the amount of the ET-1-induced Cx43-P as quantified by the Scion image analysis program.

Involvement of c-Src on ET-1-induced GJIC Reduction—Several lines of evidence demonstrated that c-Src plays a crucial role in signaling via GPCR to inactivate GJIC in Rat-1 fibroblast (20). Moreover tyrosine phosphorylation of Cx43 in cardiomyocytes was mediated by c-Src (40). Therefore, we investigated whether ET-1, through ET_AR, could induce loss of GJIC by the c-Src-mediated signaling in ovarian carcinoma cells. SL/DT experiments demonstrated that the selective Src kinase inhibitor, PP2 (50 nM), prevented the ET-1-induced reduction of GJIC in HEY cells (Fig. 7*A*). Signaling molecules involved in ET_AR-stimulated tyrosine kinase pathways include Src in different cell types (41, 42). Using specific anti-phospho-Src antibody (anti-Src ($Tyr(P)^{418}$)) (43), we found that exposure of HEY cells to ET-1 induced a time-dependent increase of c-Src kinase activation reaching a maximum after 30 min of stimulation, which concurred with kinetics of Cx43 phosphorylation (Fig. 7*B*). Moreover, pretreatment of ovarian cancer cells with PP2 (50 nM) blocked the ET-1-induced tyrosine phosphorylation of c-Src (Fig. 7*C*) and Cx43 tyrosine phosphorylation (Fig. 7*D*). Because Cx43 has been reported to interact directly with c-Src and this interaction is a necessary and sufficient condition to phosphorylate Cx43 (20), we investigated the effects of ET-1 on the Cx43 interaction with c-Src (Fig. 7*E*). ET-1 stimulation of HEY cells led to an activation of c-Src that coimmunoprecipitated with Cx43 (Fig. 7*E*), indicating c-Src as a suitable candidate for ET-1-induced GJIC inhibition and Cx43 phosphorylation.

Analysis of Cx43 Protein Expression in Ovarian Carcinoma Xenografts of Animals Treated with ET_AR Antagonist—To evaluate *in vivo* the effect of the potent ET_AR antagonist, ABT-627, we examined immunohistochemically Cx43 expression in murine ovarian carcinoma xenografts. HEY ovarian carcinoma

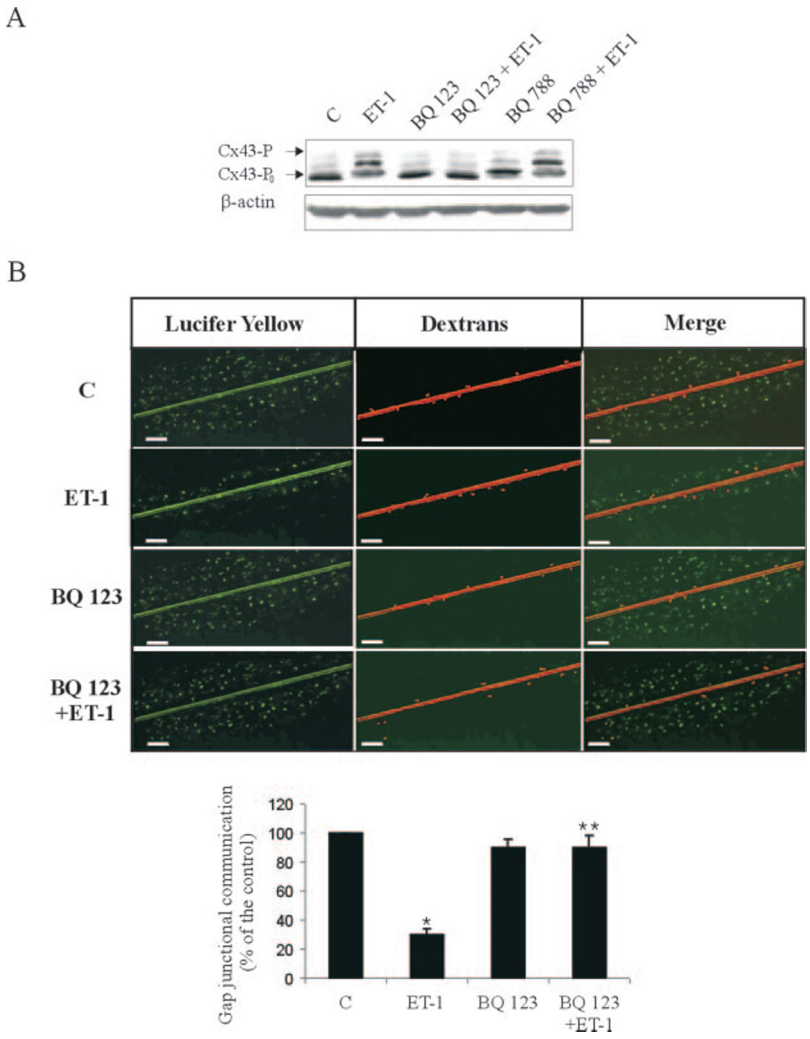

FIG. 3. **Effects of ET_AR antagonist on ET-1-induced Cx43 phosphorylation.** HEY cells were incubated for 30 min with 100 nM ET-1 in the absence or in presence of BQ 123 (1 μM) or BQ 788 (1 μM). Lysates were assayed for Cx43 expression by Western blotting. After being stripped, the membranes were reprobed with β-actin-specific antibody to ensure equal loading (*A*). ET-1 (100 nM) effects on GJIC were analyzed in HEY cells in the absence or presence of BQ123 (1 μM) by the SL/DT method, and the data were quantified as described under "Experimental Procedures" and expressed as the relative percentage of the control (*B*). The data show a representative experiment of three different experiments; results are means of triplicate samples ± S.D. *, $p <$ 0.001 compared with control; **, $p < 0.05$ compared with ET-1. *Bar* (*B*), 100 μm.

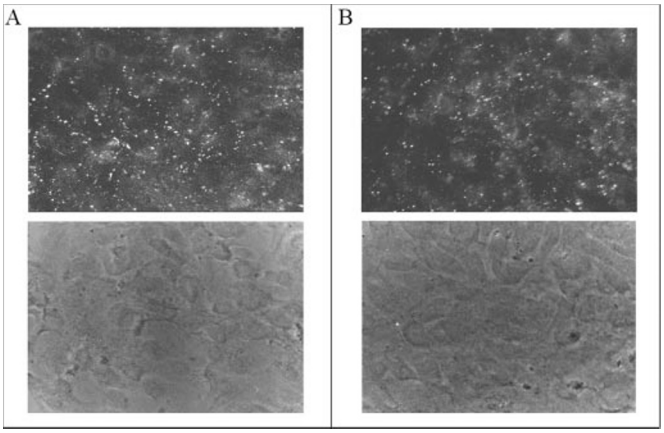

FIG. 4. **Immunolocalization of Cx43 in HEY ovarian cancer cells.** HEY cells were cultured in serum-free medium for 30 min in the absence (*A*) or in the presence (*B*) of 100 nM ET-1. Cells were immunostained by using monoclonal anti-Cx43. A fine punctate Cx43-staining characteristic of gap junctional plaques is observed at cell-cell contact areas in untreated cells. Treatment with ET-1 results in a punctate staining that appears now randomly distributed. Original magnification, ×60.

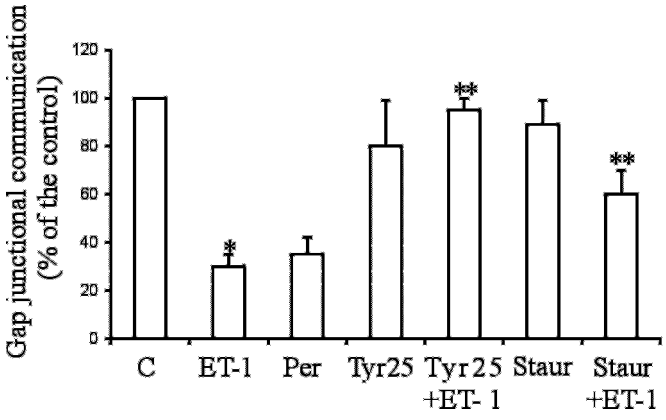

FIG. 5. **Effects of tyrosine kinase and phosphatase inhibitors.** Serum-starved HEY cells were treated with the tyrosine phosphatase inhibitor pervanadate (*Per*; 1 mM) or with ET-1 (100 nM) or pretreated for 30 min with the tyrosine kinase inhibitor tyrphostin 25 (*Tyr 25*; 100 μM) or with the Ser/Thr kinase inhibitor staurosporine (*Staur*; 100 nM) and then treated for 30 min with ET-1. GJICs were measured by the scrape-loading method. The data show a representative experiment of three different experiments; results are means of triplicate samples ± S.D. *, $p < 0.001$ compared with control; **, $p < 0.05$ compared with ET-1.

cells were grown as subcutaneous tumors in nude mice. At day 7, when well established HEY xenografts were palpable with a tumor size of ~0.25 cm^3, mice were randomized into treated and vehicle-injected control groups of 10 animals each. The treated mice were injected intraperitoneally for 21 days with 2 mg/kg/day of ABT-627. A 2 mg/kg/day dose of ABT-627 was selected because it induced a 65% inhibition of the tumor growth, was well tolerated, and corresponded to that used in human clinical trials (18). Immunohistochemical evaluation of the expression of Cx43, performed on HEY tumors at day 40 after the tumor cell injection, revealed an increase in Cx43-

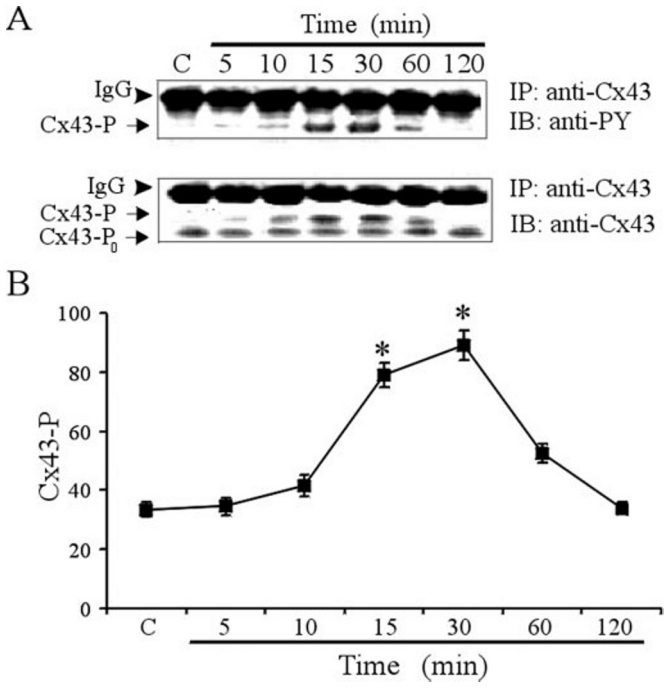

FIG. 6. **Kinetics of Cx43 tyrosine phosphorylation in HEY cells.** HEY cells were stimulated for up to 120 min with 100 nM ET-1. Cx43 was immunoprecipitated (*IP*) from cell lysates and immunoblotted (*IB*) with anti-phosphotyrosine (*anti-PY*; *upper panel*) or with anti-Cx43 (*lower panel*) in Western blot. Heavy chain of immunoglobulin (*IgG*) migrates upper tyrosine-phosphorylated Cx43 as indicated by the *arrowheads* (*A*). The relative density of Cx43-P content from *A* was statistically analyzed and represents the average value of three independent Western blots ± S.D.; *, $p < 0.001$ compared with control (*B*).

based gap junction plaques in HEY tumors treated with ABT-627 (Fig. 8*A*). Western blot analysis of the expression of Cx43 protein, performed on HEY tumor xenografts freshly excised on day 40 after tumor cell injection, revealed a marked reduction in the phosphorylated forms of Cx43 in ABT-627-treated mouse compared with control (Fig. 8*B*). To prove that the observed ABT-627-induced reduction of Cx43 phosphorylation occurs on a tyrosine residue, HEY xenograft lysates were immunoprecipitated with anti-Cx43 and immunoblotted with anti-phosphotyrosine (Fig. 8*C*). Immunoprecipitation and immunoblot analysis indicated that ABT-627 treatment resulted in a significant reduction of Cx43 tyrosine phosphorylation. These data indicate that ET_AR antagonist prevents *in vivo* Cx43 tyrosine phosphorylation and subsequent degradation related to cellular uncoupling.

DISCUSSION

During tumor progression, epithelial cancer cells leave their local "neighborhood" to move into new microenvironments by acquiring a local invasive and metastatic phenotype. The acquisition of migratory abilities in epithelial cells is accompanied by the loss of expression of cell-cell junctional molecules. Several growth factors that bind tyrosine kinase receptors or GPCR have been shown to induce deregulation or loss of function of GJIC in several cell types by inducing Cx43 phosphorylation (20, 24–26, 40). In the present study, we demonstrated that in ovarian carcinoma cells, ET-1 via ET_AR induces a transient and a dose-dependent reduction of GJIC. Western blot and immunolocalization analysis clearly showed that Cx43 become more phosphorylated, and fewer gap junction plaques were apparent when ovarian cancer cells were treated with ET-1, suggesting that ET-1 promotes the cellular uncoupling at

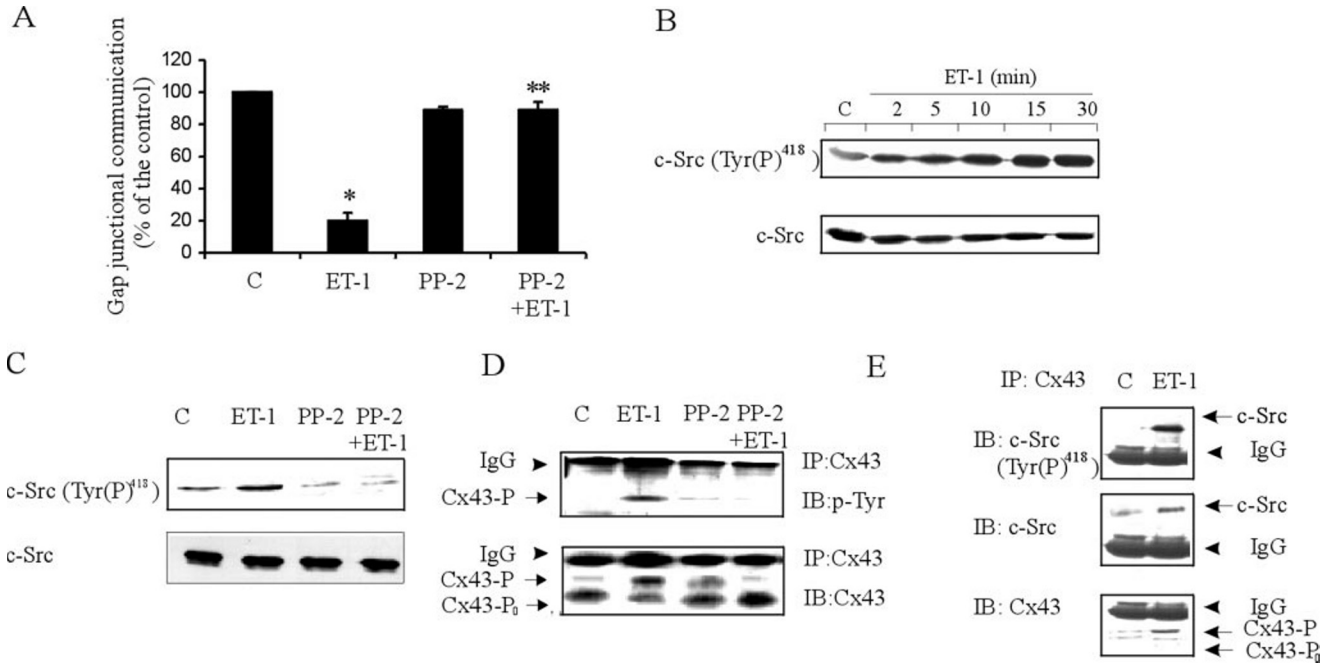

FIG. 7. **Involvement of protein-tyrosine kinase c-Src on ET-1 effects.** *A*, HEY cells were pretreated for 30 min with the c-Src inhibitor PP2 (50 nM) and then treated with 100 nM ET-1 for 30 min. GJICs were measured by the SL/DT method, and the data were quantified and expressed as the relative percentage of the control. The data show a representative experiment of three different experiments, and results are means of triplicate samples ± S.D. Statistical comparisons were made in reference to untreated cells. *, $p < 0.001$ compared with control; **, $p < 0.05$ compared with ET-1. *B*, HEY cells were stimulated with 100 nM ET-1 for the indicated time periods. The activated form of c-Src was detected by using specific anti-c-Src (Tyr(P)^{418}), and total c-Src was detected by using anti-c-Src (*lower panel*). *C*, whole cell lysates from HEY cells treated with ET-1 (100 nM) or PP2 (50 μM) alone or in combination with ET-1 were immunoblotted (*IB*) with specific anti-c-Src (Tyr(P)^{418}; *upper panel*) or total c-Src by using anti-c-Src (*lower panel*). *D*, the same lysates as in *C* were immunoprecipitated (*IP*) with anti-Cx43 and immunoblotted either with anti-phosphotyrosine (*upper panel*) or with anti-Cx43 (*lower panel*). *E*, cell lysates from ET-1-treated and untreated HEY cells were immunoprecipitated with anti-Cx43 and immunoblotted with anti-c-Src (Tyr(P)^{418}; *upper panel*), anti-c-Src (*middle panel*), or anti-Cx43 (*lower panel*). The positions of c-Src and c-Src (Tyr(P)^{418}) are indicated by the *arrows*. In *D* and *E*, heavy chain of immunoglobulin (*IgG*) is indicated by the *arrowheads*.

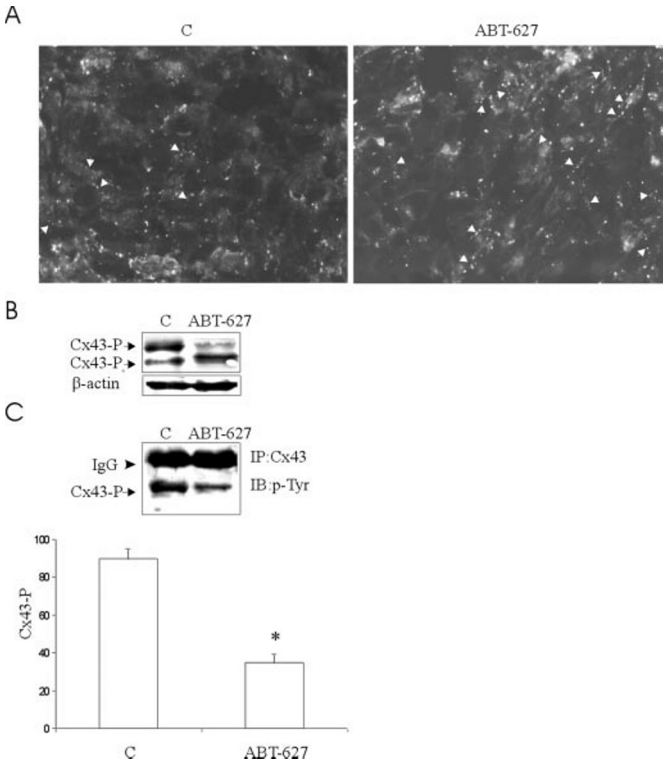

FIG. 8. **ABT-627, the ET_AR antagonist, blocks ET-1-mediated effects *in vivo*.** *A*, expression of Cx43 in HEY tumor xenografts of control and ABT 627-treated mice. Animals bearing HEY tumor xenografts were treated intraperitoneally for 21 days with ABT-627 (2 mg/kg/day). Tumors were removed from controls and from treated mice and were snap-frozen in liquid nitrogen on day 40 after tumor injection. Indirect immunofluorescence on 4-μm acetone-fixed cryostat sections employing rabbit anti-Cx43 antiserum was performed for expression of Cx43. Whereas in control the fine punctate staining is randomly distributed, in tumors of treated animals the staining is frequently arranged in plaques (*arrowheads*) (original magnification, $\times$60). *B*, Western blot analysis of total cell lysates obtained from freshly excised tumor. An equal amount of protein lysates from untreated mice or ABT-627-treated mice were subjected to Western blot and analyzed for Cx43 expression with anti-Cx43. After being stripped, the membranes were reprobed with β-actin-specific antibody to ensure equal loading. *C*, Cx43 was immunoprecipitated (*IP*) from HEY xenograft lysates and immunoblotted (*IB*) with anti-phosphotyrosine (*anti-PY*) in Western blot. Heavy chain of immunoglobulin (*IgG*) migrates upper tyrosine-phosphorylated Cx43 as indicated by the *arrowheads*. The relative density of Cx43-P content from *C* was statistically analyzed and represents the average value of three independent Western blots $\pm$ S.D. *, $p < 0.001$ compared with control.

the level of connexin maturation and subsequent degradation. Cx43 tyrosine phosphorylation was mainly responsible for ET-1-induced loss of cell-cell communication in these tumor cells as demonstrated by experiments performed with specific tyrosine kinase inhibitor that prevented the ET-1-induced GJIC reduction and with an inhibitor of tyrosine phosphatase that mimicked the ET-1 action on GJIC. These is supported further by Postma *et al.* (20), who demonstrated that GPCR agonists, such as ET-1, transiently disrupt GJIC in Rat-1 cells through a tyrosine kinase pathway and that GPCR use c-Src kinase to inhibit Cx43-based cell-cell communication. The present data demonstrate that ET-1 rapidly activates c-Src and that this tyrosine kinase could represent a potential mediator of ET-1 effects on ovarian carcinoma cells. Analysis of the ET-1 signaling by the specific inhibitor of c-Src strongly suggests that the ET-1-induced Cx43 phosphorylation and GJIC reduction is likely to be mediated by the c-Src tyrosine kinase pathway. ET-1-induced cellular uncoupling was partially inhibited by staurosporine, a protein kinase C inhibitor, suggesting that ET-1-induced breakdown of communication is mediated by one or more protein kinases that include both tyrosine kinase, such as c-Src, and serine/threonine kinases, such as protein kinase C or mitogen-activated protein kinase, which are both activated by ET-1 in these ovarian carcinoma cells (11). The latter findings parallel those of Polontchouch *et al.* (21), demonstrating that ET-1 induces Cx43 phosphorylation *in vitro* through mitogen-activated protein kinase signaling pathways in cardiomyocyte.

Degradation of phosphorylated Cx43 has been reported to be correlated with the rapid turnover/disassembly of gap junction plaques, with the consequent decrease in intercellular communication (27). Data presented in this study cannot exclude the possibility that ET-1-induced Cx43 phosphorylation could destabilize gap junction plaques by a mechanism involving the degradation pathway. The intrinsic mechanism whereby Cx43 gets targeted for degradation in response to ET-1-induced phosphorylation remains to be investigated in future studies.

Interestingly, we found that addition of a specific ET_AR antagonist, BQ 123, blocked the ET-1-induced loss of GJIC and Cx43 phosphorylation, demonstrating that ET_AR activation by ET-1 contributes to loss of growth control via a Cx43-mediated disruption of GJIC. In a previous study, we demonstrated that ET_AR blockade by the potent ET_AR antagonist, ABT-627, resulted in therapeutic activity against established ovarian carcinoma expressing ET_AR. This effect was associated with a significant decrease in microvessel density and in vascular endothelial growth factor and matrix metalloproteinase-2 expression and with an increased percentage of apoptotic cells (18). In this study, we found that ABT-627 treatment, concomitantly with a reduction of tumor growth, increases the Cx43-based gap junction plaques and decreases Cx43 tyrosine phosphorylation, indicating that the antitumoral activity of ABT-627 may also be due to the prevention of post-transcriptional modification of Cx43. In addition to its well established role as a channel-forming protein, Cx43 might function as a microtubule-anchoring protein (44). In this model, it has been proposed that Cx43 is part of a multiprotein complex. For example, the c-Src can bind directly and phosphorylate the Cx43, a mechanism that seems responsible for the disruption of Cx43 interaction with the scaffolding protein zona occludens protein 1 (ZO-1), which associates with tight junction, cytoskeleton, and signal transduction molecules in several cell types (45–47). Recent results demonstrated that c-Src acts by affecting trafficking of Cx43 to the plasma membrane or by altering connexin-connexin assembly within the plasma membrane through regulation of the Cx43-ZO-1 interaction. Thus, the cytoplasmatic-terminal region of Cx43 is also a multimeric interaction site for cytoskeleton structures like ZO-1. Cx43 is also directly stimulated by Wnt-1 signaling (48) and can interact with the adherens junction protein, β-catenin (49). It has been demonstrated that restoration of cadherin-based cell-cell adhesion induces the assembly of Cxs into gap junctions (50). Similarly, in prostate cancer cells, α-catenin expression triggered the trafficking and assembly of Cxs into gap junctions and recruited ZO-1 to the cell surface (51). The significance of this finding is not understood. Because the dynamic behavior of cell interactions and communication is affected in migrating cells that lack cell-cell contacts, one can envision that a GPCR, such as ET_AR, which mediated inhibition of Cx43-based junctional communication, might alter intercellular interactions that are responsible for contact-mediated regulatory control. The molecular mechanisms by which cadherins and their associated proteins may facilitate the assembly of Cxs into gap junctions are likely to be complex. The possibility that ET-1 alters cell adhesion and that it consequently alters the assem-

bly of Cxs into gap junction remains to be explored in the future in light of the dynamic nature of cell-cell adhesion induced by ET-1. The capacity of ET-1 to disrupt gap junctions through phosphorylation of Cx43 via c-Src described here could serve as a basis to further evaluate the cell-cell metabolic uncoupling and cell detachment that occurs during tumor progression and add further information on the overall relevance of ET_AR in regulating the complex assay of cell-cell or cell-matrix interactions promoting ovarian carcinoma growth. Interestingly, the ovarian cancer cells that expressed ET_AR showed multiple aggressive parameters including the ability to down-regulate E-cadherin-mediated adhesive interactions.[2] Here, we demonstrated that ABT-627 is able to block Cx43 tyrosine phosphorylation and to increase Cx43-based intercellular communication, which are correlated with tumor growth reduction in ovarian carcinoma xenografts. New therapeutic strategies using specific ET_AR antagonists with suitable pharmacological and toxicity profiles for clinical use (36, 37) may provide a novel approach to the treatment of ovarian carcinoma in which ET_AR blockade could result in tumor growth inhibition also by preventing the disruption of cell-cell communication.

Acknowledgments—We gratefully acknowledge Dr. Perry Nisen (Global Oncology Development) of Abbott for kindly providing the ABT-627, Marco Varmi and Giacomo Elia for excellent technical assistance, and Maria Vincenza Sarcone for secretarial assistance.

REFERENCES

1. Nelson, J. B., Hedican, S. P., George, D. J., Reddi, A. H., Piantadosi, S., Eisenberger, M. A., and Simons J. W. (1995) *Nat. Med.* **1,** 994–999
2. Bagnato, A., Tecce, R., Moretti, C., Di Castro, V., Spergel, D., and Catt, K. J. (1995) *Clin. Cancer Res.* **1,** 1059–1066
3. Bagnato, A., Salani, D., Di Castro, V., Wu-Wong, J. R., Tecce, R., Nicotra, M. R., Venuti, A., and Natali, P. G. (1999) *Cancer Res.* **59,** 720–727
4. Egidy, G., Juillerat-Jeanneret, L., Jeannin, J. F., Korth, P., Bosman, F. T., and Pinet, F. (2000) *Am. J. Pathol.* **157,** 1863–1874
5. Venuti, A., Salani, D., Manni, V., Poggiali, F., and Bagnato, A. (2000) *FASEB J.* **14,** 2277–2283
6. Baley, P. A., Resink, T. J., Eppenberger, U., and Hahn, A. W. (1990) *J. Clin. Invest.* **85,** 1320–1323
7. Economos, K., MacDonald, P. C., and Casey, M. L. (1992) *Cancer Res.* **52,** 554–557
8. Lahav, R., Heffner, G., and Patterson, P. H. (1999) *Proc. Natl. Acad. Sci. U. S. A.* **96,** 11496–11500
9. Bagnato, A., Rosanò, L., Di Castro, V., Albini, A., Salani, D., Varmi, M., Nicotra, M. R., and Natali, P. G. (2001) *Am. J. Pathol.* **158,** 841–847
10. Rubanji, G. M., and Polokoff, M. A. (1999) *Pharmacol. Rev.* **46,** 325–414
11. Nelson, J. B., Bagnato, A., Battistini, B., and Nisen, P. (2003) *Nat. Rev. Cancer* **3,** 110–116
12. Bagnato, A., Tecce, R., Di Castro, V., and Catt, K. J. (1997) *Cancer Res.* **57,** 1306–1311
13. Del Bufalo, D., Di Castro, V., Biroccio, A., Varmi, M., Salani, D., Rosano, L., Trisciuoglio, D., Spinella, F., and Bagnato, A. (2002) *Mol. Pharmacol.* **61,** 524–532
14. Rosanò, L., Varmi, M., Salani, D., Di Castro, V., Spinella, F., Natali, P. G., and Bagnato, A. (2001) *Cancer Res.* **61,** 8340–8346
15. Salani, D., Di Castro, V., Nicotra, M. R., Rosanò, L., Tecce, R., Venuti, A., Natali, P. G., and Bagnato, A. (2000) *Am. J. Pathol.* **157,** 1537–1547
16. Salani, D., Taraboletti, G., Rosanò, L., Di Castro, V., Borsotti, P., Giavazzi, R., and Bagnato, A. (2000) *Am. J. Pathol.* **157,** 1703–1711
17. Spinella, S., Rosanò, L., Di Castro, V., Natali, P. G., and Bagnato, A. (2002) *J. Biol. Chem.* **277,** 27850–27855
18. Rosanò, L., Spinella, F., Salani, D., Di Castro, V., Venuti, A., Nicotra, M. R., Natali, P. G., and Bagnato, A. (2003) *Cancer Res.* **63,** 2447–2453
19. Blomstrand, F., Giaume, C., Hansson, E., and Ronnback, L. (1999) *Am. J. Physiol.* **277,** C616–C627
20. Postma, F. R., Hengeveld, T., Alblas, J., Giepmans, B. N., Zondag, G. C., Jalink, K., and Moolenaar, W. H. (1998) *J. Cell Biol.* **140,** 1199–1209
21. Polontchouk, L., Ebelt, B., Jackels, M., and Dhein, S. (2002) *FASEB J.* **16,** 87–89
22. Goodenough, D. A., Goliger, J. A., and Paul, D. L. (1996) *Ann. Rev. Biochem.* **65,** 475–502
23. Trosko, J. E., and Chang, C. C. (2001) *Mutat. Res.* **1,** 219–229
24. Ruch, R. J., Trosko, J. E., and Madhukar, B. V. (2001) *J. Cell. Biochem.* **83,** 163–169
25. Lidington, D., Tyml, K., and Ouellette, Y. (2002) *J. Cell. Physiol.* **193,** 373–379
26. Cruciani, V., and Mikalsen, S. O. (2002) *Biol. Cell* **94,** 433–443
27. Lampe, P. D., and Lau, A. F. (2000) *Arch. Biochem. Biophys.* **384,** 205–215
28. Laing, J. G., Tadros, P. N., Westphale, E. M., and Beyer, E. C. (1997) *Exp. Cell Res.* **236,** 482–492
29. Hanna, E. A., Umhauer, S., Roshong, S. L., Piechocki, M. P., Fernstrom, M. J., Fanning, J. D., and Ruch, R. J. (1999) *Carcinogenesis* **20,** 1369–1373
30. Umhauer, S., Ruch, R. J., and Fanning, J. (2000) *Am. J. Obstet. Gynecol.* **182,** 999–1000
31. Fernstrom, M. J., Koffler, L. D., Abou-Rjaily, G., Boucher, P. D., Shewach, D. S., and Ruch, R. J. (2002) *Exp. Mol. Pathol.* **73,** 54–60
32. Auersperg, N., Wong, A. S., Choi, K. C., Kang, S. K., and Leung, P. C. (2001) *Endocr. Rev.* **22,** 255–288
33. Darai, E., Scoazec, J. Y., Walker-Combrouze, F., Mlika-Cabanne, N., Feldmann, G., Madelenat, P., and Potet, F. (1997) *Hum. Pathol.* **28,** 922–928
34. Salani, D., Rosanò, L., Di Castro, V., Spinella, F., Venuti, A., Padley, R. J., Nicotra, M. R., Natali, P. G., and Bagnato, A. (2002) *Clin. Sci. (Lond.)* **103,** (suppl.) 318S–321S
35. Bagnato, A., Cirilli, A., Salani, D., Simeone, P., Muller, A., Nicotra, M. R., Natali, P. G., and Venuti, A. (2002) *Cancer Res.* **62**, 6381–6384
36. Van der Boon, J. (2002) *Lancet Oncol.* **3,** 201
37. Carducci, M. A., Nelson, J. B., Bowling, M. K., Rogers, T., Eisenberger, M. A., Sinibaldi, V., Donehower, R., Leahy, T. L., Carr, R. A., Isaacson, J. D., Janus, T. J., Andre, A., Hosmane, B. S., and Padley, R. J. (2002) *J. Clin. Oncol.* **20,** 2171–2180
38. Carruba, G., Webber, M. M., Quadre, S. T., Amoroso, M., Cocciadiferro, L., Saladino, F., Trosko, J. E., and Castagnetta, L. A. (2002) *Prostata* **50,** 73–82
39. Musil, L. S., Beyer, E. C., and Goodenough, D. A. (1990) *J. Membr. Biol.* **116,** 163–175
40. Toyofuku, T., Akamatsu, Y., Zhang, H., Kuzuya, T., Tada, M., and Hori, M. (2001) *J. Biol. Chem.* **276,** 1780–1788
41. Simonson, M. S., Wang, Y., and Herman, H. (1996) *J. Biol. Chem.* **271,** 77–82
42. Sumimoto, M., Milowsky, M. I., Shen, R., Navarro, D., Dai, J., Asano, T., Hayakawa, M., and Nanus, D. M. (2001) *Cancer Res.* **61,** 3294–3298
43. Giusti, A. F., Xu, W., Hinkle, B., Terasaki, M., and Jaffe, L. A. (2000) *J. Biol. Chem.* **275,** 16788–16794
44. Giepmans, B. N., Verlaan, I., Hengeveld, T., Janssen, H., Calafat, J., Falk, M. M., and Moolenaar, W. H. (2001) *Curr. Biol.* **11,** 1364–1368
45. Giepmans, B. N., and Moolenaar, W. H. (1998) *Curr. Biol.* **8,** 931–934
46. Giepmans, B. N., Verlaan, I., and Moolenaar, W. H. (2001) *Cell Commun. Adhes.* **8,** 219–223
47. Laing, J. G., Manley-Markowski, R. N., Koval, M., Civitelli, R., and Steinberg, T. H. (2001) *J. Biol. Chem.* **276,** 23051–23055
48. Van der Heyden, M. A., Rook, M. B., Hermans, M. M., Rijksen, G., Boonstra, J., Defize, L. H., and Destree, O. H. (1998) *J. Cell Sci.* **111,** 1741–1749
49. Ai, Z., Fischer, A., Spray, D. C., Brown, A. M., and Fishman, G. I. (2000) *J. Clin. Invest.* **105,** 161–171
50. Musil, L. S., Cunningham, B. A., Edelman, G. M., and Goodenough, D. A. (1990) *J. Cell Biol.* **111,** 2077–2088
51. Govindarajan, R., Zhao, S., Song, X. H., Guo, R. J., Wheelock, M., Johnson, K. R., and Mehta, P. P. (2002) *J. Biol. Chem.* **277,** 50087–50097

[2] L. Rosanò, F. Spinella, V. D. Castro, P. G. Natali, and A. Bagnato, unpublished results.